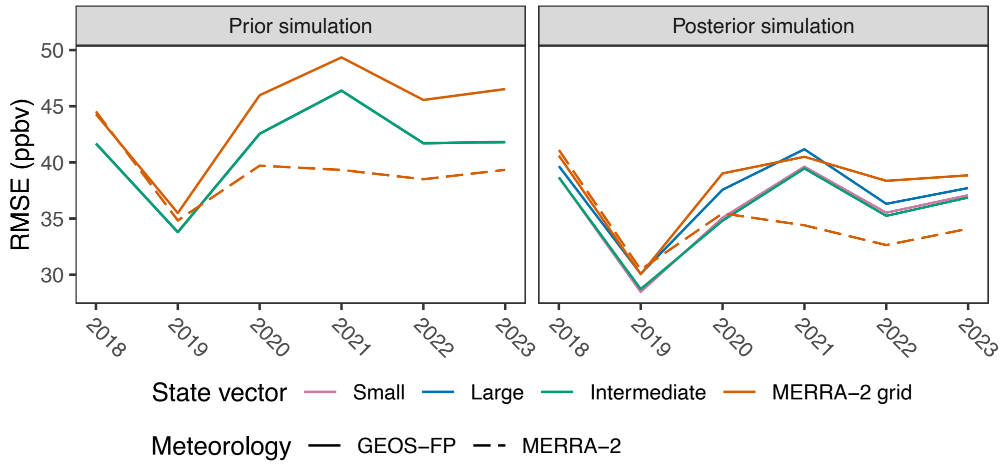

Figure S1. Annual root mean square error (RMSE) within NYS of prior and posterior simulations from ensembles assimilating only afternoon observations. In the prior simulation subplot, the ensemble using the intermediate state vector (green) overplots the ensembles using the small and large state vectors because changing only state vector selection at a given model resolution does not impact the prior simulation. Comparison of the ensembles using the coarser-resolution MERRA-2 grid (orange), which differ only in meteorological fields, reveals a decrease in model performance in the prior simulations using GEOS-FP meteorology beginning in 2020 that is reflected in the posterior simulations.

Table S1. Summary of ensemble performance and information content for New York State (NYS) inversions. Columns report the mean bias (ppbv) in synthetic methane observations across all sites, along with the root mean square error (RMSE) in ppbv in synthetic methane observations at NYS sites and across all sites. Ensembles that assimilate only afternoon observations exhibit the smallest absolute mean biases and the smallest RMSE both within NYS and across all observation sites.

Meteorology	Boundary conditions	Observation time	Sites	State vector	Time range	Mean bias All sites	RMSE NYS sites	RMSE All sites
GEOS-FP	CarbonTracker-CH_4	Afternoon[b]	All	Default	2018-2023	-4.4	35.91	41.27
GEOS-FP	CarbonTracker-CH_4	Afternoon	All	Rectangular	2018-2023	-4.2	37.28	39.71
GEOS-FP	CarbonTracker-CH_4	Afternoon	All	Obs.-Emis.[c]	2018-2023	-3.0	35.79	39.11
GEOS-FP	CarbonTracker-CH_4	Afternoon	All	MERRA-2 Grid	2018-2023	-4.8	38.07	43.46
MERRA-2	CarbonTracker-CH_4	Afternoon	All	MERRA-2 Grid	2018-2023	-6.2	34.82	42.13
GEOS-FP	TROPOMI+GOSAT	Afternoon	All	Default	2018-2024[d]	-4.3	40.30	46.32
GEOS-FP	CarbonTracker-CH_4	All	All	Default	2018-2023	-10.2	52.76	62.47
GEOS-FP	CarbonTracker-CH_4	All	All	Rectangular	2018-2023	-10.0	55.06	61.75
GEOS-FP	CarbonTracker-CH_4	All	All	Obs.-Emis.	2018-2023	-6.4	52.80	59.25
GEOS-FP	CarbonTracker-CH_4	Afternoon	UR+ECCC[e]	Default	2018-2023[f]	1.7	38.37	36.48
GEOS-FP	CarbonTracker-CH_4	Afternoon	UR+ECCC	Rectangular	2018-2023[g]	-3.2	36.66	35.34

[b] 12:00-14:59 Local Time
[c] Observations-Emissions
[d] Mean bias and RMSE reported for 2020-2024 only
[e] WHT, EGB, DWS, ROC, PSP, LDO; see Table 2
[f] Mean bias and RMSE reported for 2019 and 2021 only
[g] Mean bias and RMSE reported for 2019 and 2021-2023 only

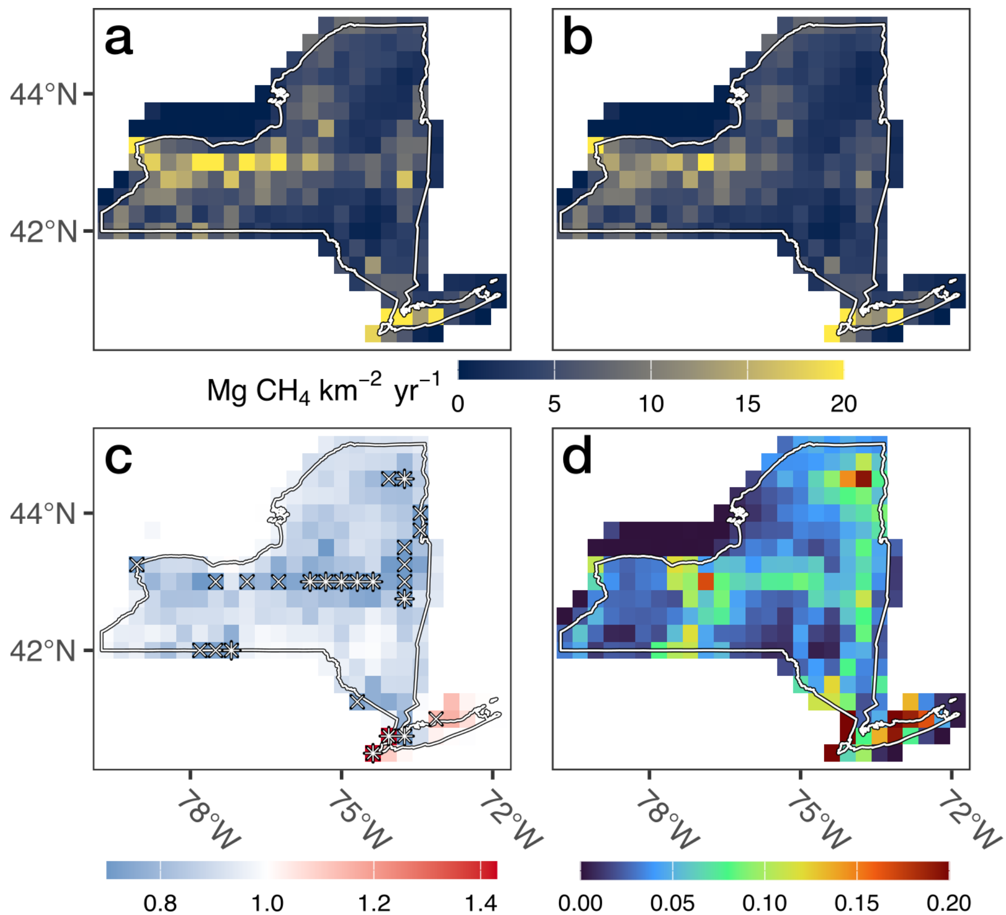

Figure S2. Prior and optimized emissions from the ensemble using the small state vector and assimilating only afternoon observations. (a) Mean total prior emissions across all years; (b) Mean total posterior emissions across all years; scaling factor mean (c) and standard deviation (d) across years of the ensemble. Statistically significant scaling factors in at least one year and at least three years are represented in (c) by grid cells overlaid with × and ∗, respectively.

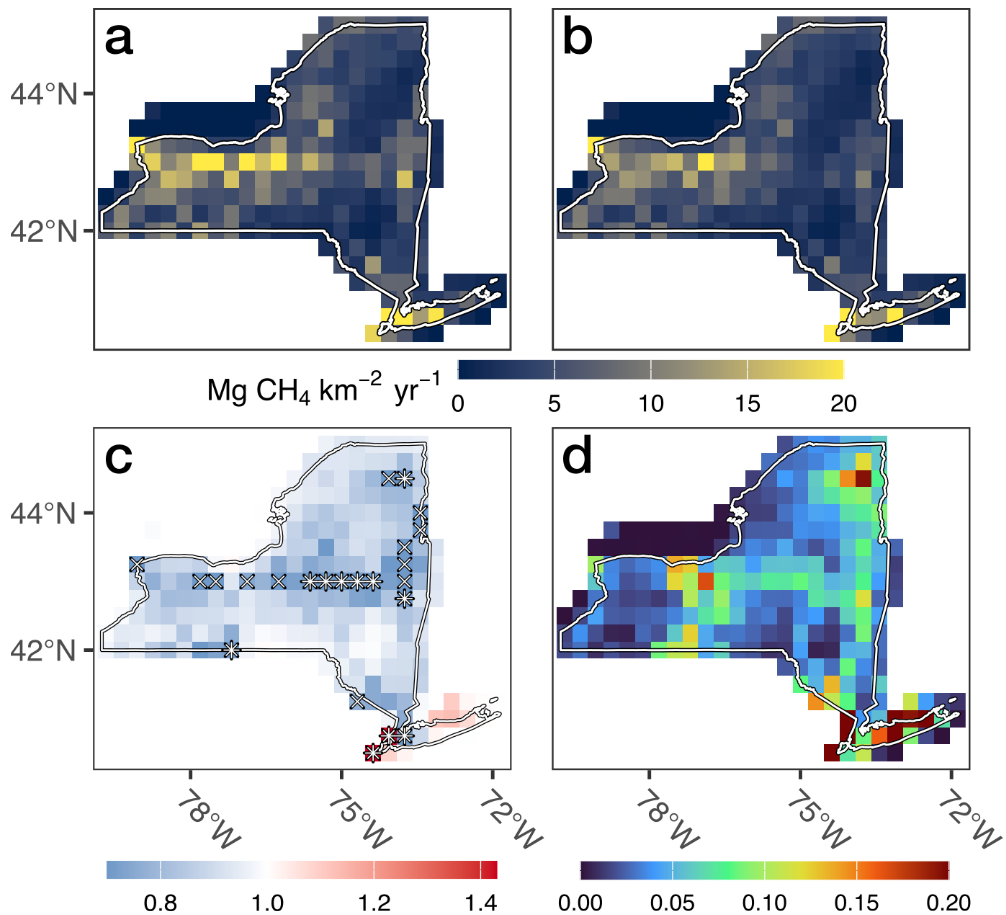

Figure S3. Prior and optimized emissions from the ensemble using the intermediate state vector and assimilating only afternoon observations. (a) Mean total prior emissions across all years; (b) Mean total posterior emissions across all years; scaling factor mean (c) and standard deviation (d) across years of the ensemble. Statistically significant scaling factors in at least one year and at least three years are represented in (c) by grid cells overlaid with × and ∗, respectively.

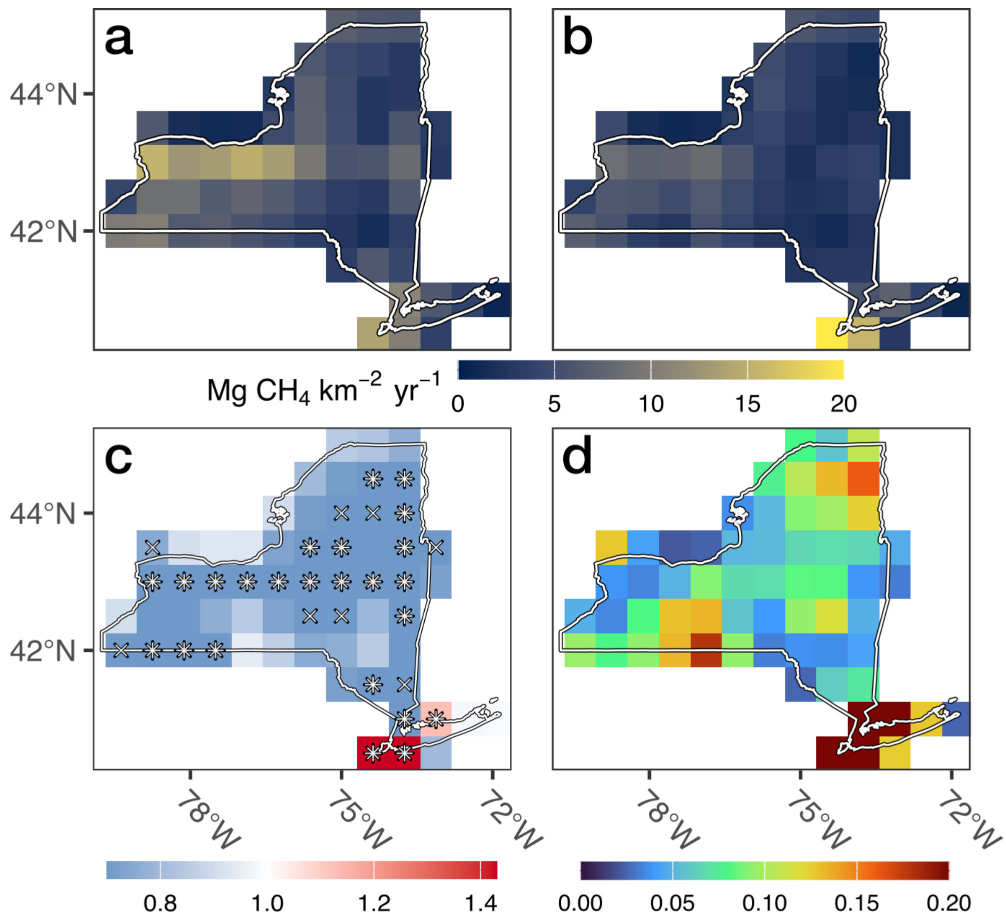

Figure S4. Prior and optimized emissions from the ensemble using the coarser MERRA-2 grid state vector and assimilating only afternoon observations. (a) Mean total prior emissions across all years; (b) Mean total posterior emissions across all years; scaling factor mean (c) and standard deviation (d) across years of the ensemble. Statistically significant scaling factors in at least one year and at least three years are represented in (c) by grid cells overlaid with × and ∗, respectively.

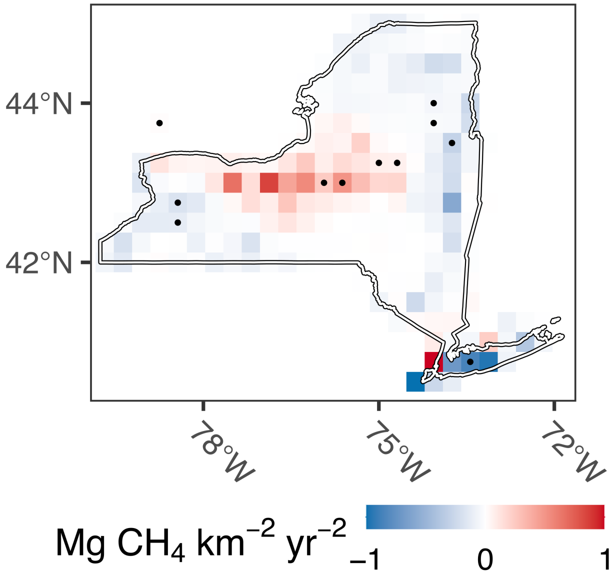

Figure S5. Interannual trends in posterior methane emissions can be seen in areas of southwestern, northeastern, and central NYS, as well as Long Island in the southeast. Stippling indicates statistically significant trends ($p < 0.05$) in the least squares model weighted by posterior uncertainty. Results shown for the ensemble using the small state vector and assimilating only afternoon observations.

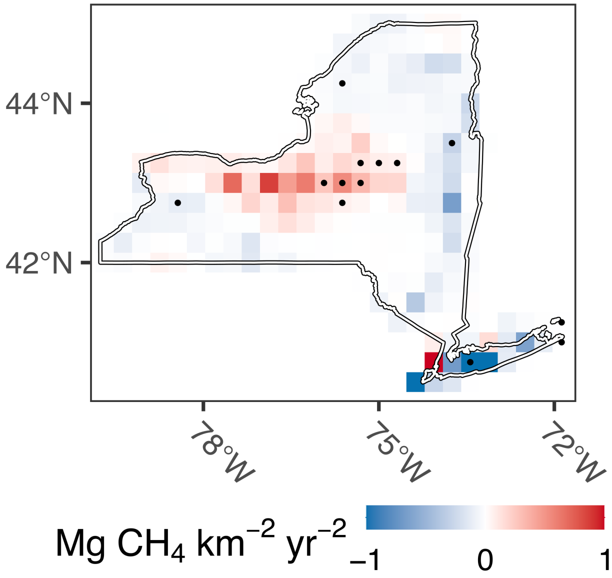

Figure S6. Interannual trends in posterior methane emissions can be seen in areas of southwestern, northeastern, and central NYS, as well as Long Island in the southeast. Stippling indicates statistically significant trends ($p < 0.05$) in the least squares model weighted by posterior uncertainty. Results shown for the ensemble using the intermediate state vector and assimilating only afternoon observations.

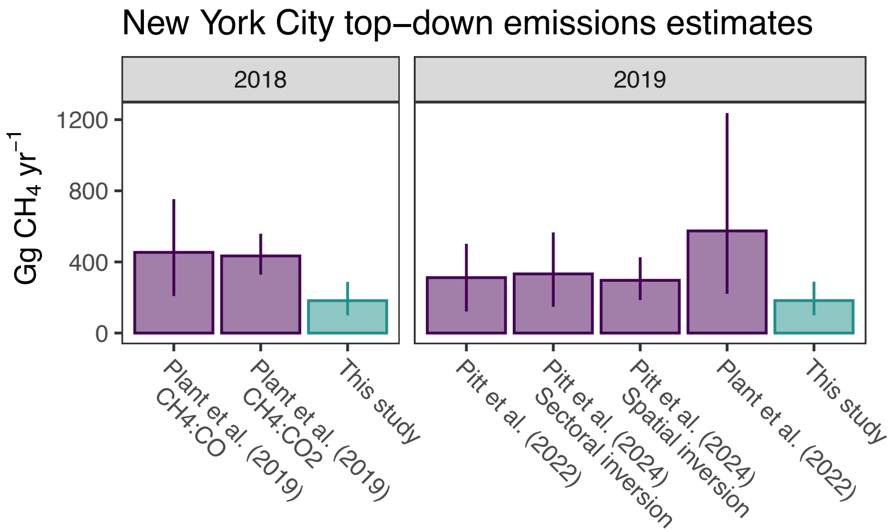

Figure S7. Total estimated emissions (Gg CH_4 year^{-1}) and 95 % confidence intervals (CI) for the New York City Metropolitan Area in select studies and the ensemble using the large state vector and assimilating all observations. Studies with observations taken in multiple years are grouped in the year containing the majority of observations.

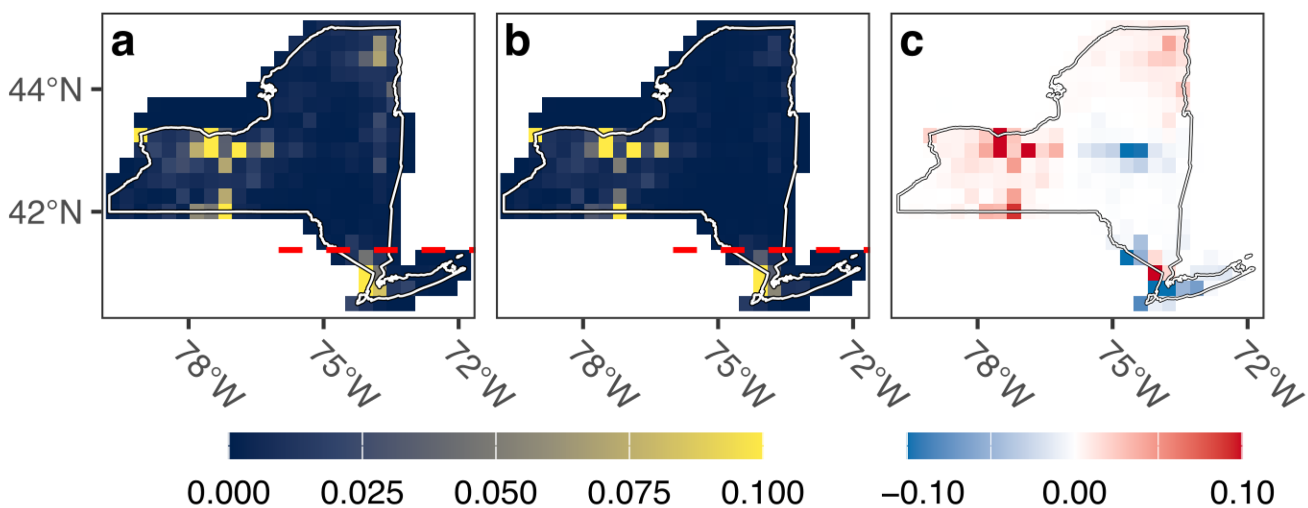

Figure S8. Reduction in information content associated with a reduced observation network using the small state vector, shown by (a) the interannual mean, (b) standard deviation, and (c) change in interannual mean of the averaging-kernel diagonal relative to the ensemble using the small state vector and assimilating only afternoon observations from all sites. Grid cells below the dashed red line are centered south of $41.375°$N. Positive differences indicate locations where the removal of observational constraints reduces the influence of competing information from other sites, rather than reflecting an improvement in observational sensitivity.